

# A Comparison Between the Heating Process of the Therapeutic Ultrasound and Infrared Radiation Applied in Physical Therapy Using PVCP Phantoms

Gabriela Beatriz Gomes, Lucas Lobianco De Matheo, Thais Pionório Omena, Thuane Abdala, Marco Antonio von Kruger, and Wagner Coelho de Albuquerque Pereira

## Abstract

This paper aims to compare the so-called superficial heating methods used in Physical Therapy by comparing the therapeutic ultrasound and the infrared radiation, both considered superficial thermotherapeutic equipment. Thermotherapy is a therapeutic modality that promotes several health benefits. However, there are gaps in scientific knowledge regarding these techniques when applied to physical therapy and its clinical use. So, a Polyvinylchloride plastisol phantom was used to mimic the acoustic properties of soft tissues. The experimental setup was composed of a 3-MHz ultrasound equipment, and an infrared lamp. In the ultrasound protocol the nominal intensity of  $1.0 \text{ W/cm}^2$ , continuous mode was applied during one minute ( $n = 10$ ). In the infrared protocol, the phantom was positioned 30 cm apart from the infrared lamp during 15 min ( $n = 10$ ). The infrared camera remained fixed in both protocols. After comparing the heating protocols, it was observed that the infrared radiation predominantly heated the upper surface of the phantom as it was directly irradiated by the lamp. The heat was probably transferred to the deeper and adjacent layers by conduction. The ultrasound radiation at 3 MHz, heated deeper sites of the phantom than the infrared radiation and had a predominantly heating pattern along the propagation axis of the ultrasonic beam, (i.e. in the central region of the phantom). The heating pattern contributes to understand the difference between both methods, and this work proposes a new approach to superficial heating studies related to physiotherapy equipment, an area that deserves more attention of the physical principles used in the clinic.

## Keywords

Ultrasound • Infrared • Heating • Physiotherapy • Physical therapy • Phantom

## 1 Introduction

Thermotherapy is a therapeutic modality that promotes vasodilation, muscle relaxation, improvement of metabolism and local circulation, extensibility of soft tissues, alteration of tissue viscoelastic properties and reduction of inflammation [1]. In Physical Therapy, several therapeutical resources are used to heat tissues, among them one can find the Therapeutic Ultrasound (TUS) and Infrared Radiation (IRR). Ultrasound is defined as an acoustic waveform whose frequencies are higher than 20 kHz. The first application of ultrasound was in the 50's, since then it has been evolving rapidly. The TUS is one of the most used resources by physiotherapists, being applied for the treatment of a wide variety of diseases [2]. Ultrasonic waves can be delivered to the tissues in a continuous or pulsed emission, both modes results in the conversion of mechanical energy into heat [3]. However, the thermal effects produced by continuous ultrasound occur through the constant mechanical vibration of the impinged tissues. In the pulsed mode, the emission is interrupted by intercalating pauses, so the heat is dissipated by conduction reducing the production of the thermal effects [4]. The transducers frequencies range between 0.5 to 5 MHz, being 1 and 3 MHz the most used ones in clinics. The frequency of 3 MHz has a superficial effect, when compared to the frequency of 1 MHz due to the greater attenuation of higher frequencies through the medium, delivering energy in the more superficial tissues.

Infrared radiation is a physiotherapeutic method used for surface heating, acting by electromagnetic radiation, whose wavelength is between 760 and 780 nm. Like other physiotherapeutic heating methods, infrared light causes generalized vasodilatation that leads to the increment of body

G. B. Gomes (✉) · L. L. De Matheo · T. P. Omena · T. Abdala · M. A. von Kruger · W. C. de Albuquerque Pereira  
Universidade Federal do Rio de Janeiro, Rio de Janeiro, Brazil  
e-mail: [gabi.beatriz@hotmail.com](mailto:gabi.beatriz@hotmail.com)

temperature and subsequent sedation by rising the nervous depolarization threshold [5]. Infrared radiation is used for pain relief, to relax muscle stiffness, increase joint mobility, promote the regeneration of soft tissue lesions and also to skin disorders [6]. IRR can be reflected, absorbed, transmitted and subjected to refraction and diffraction by matter, which has the absorption as the process of greatest biological and clinical significance for therapeutic purposes. The biological changes promoted by IRR depend on the interaction of radiation with tissues. Since this interaction will model the penetration of energy in tissues [7]. Therefore, the penetration depends both on the absorption properties of the skin and its microstructure. Although the level of heating produced in the tissue can be estimated mathematically or can be recorded by heat sensors, in clinical practice it is common to estimate the surface heating level according to the patient's sensory report. The amount of energy received by the patient in clinics is a function of the lamp power (in Watts), distance between the lamp and patient and the duration of the treatment [8].

Although the two methods described above are widely used in Physiotherapy to delivery heat on the surface of the tissues, information regarding the degree of heating as the temperature produced by the procedure and the depth of heating is not clearly defined in the literature. Thereby, the precise tissues affected by those methods are unknown and therefore the use of them may be ineffective or even harmful.

Therefore, the objective of this work is to compare the superficial heating resources used in Physical Therapy: therapeutic ultrasound and infrared radiation. To do so, a PVCP (Polyvinylchloride plastisol) phantom was used, a material known to mimic the acoustic properties of soft tissues [9, 10].

## 2 Methods

### 2.1 Construction of the Phantom

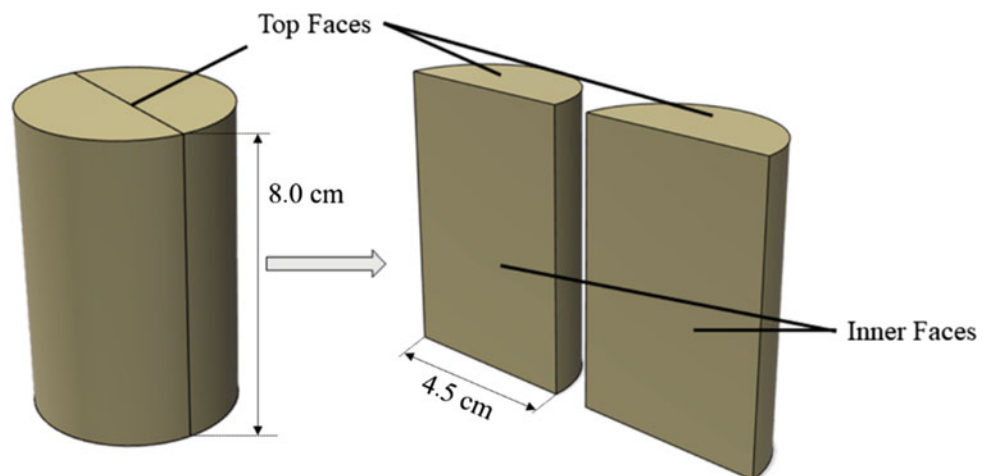
PVCP (M-F manufacturing co, Fort Worth, Texas, USA) is composed of Vinyl chloride (PVC) monomers immersed in the plasticizer. The PVCP is insoluble in water and changes its liquid state to solid state when heated over 170 °C and allowed to cool to room temperature. It is a non-toxic plastic, durable, environment and microbial agents resistant, easy to prepare and store. It has a longitudinal velocity propagation ( $1,400 \text{ m s}^{-1}$ ) and attenuation coefficient ( $0.38 \text{ dB cm}^{-1}$ ) respectively similar to fat,  $1,465 \text{ m s}^{-1}$  and  $0.4 \text{ dB cm}^{-1} \text{ MHz}^{-1}$ , [9, 10]. Using this procedure, a cylindrical phantom composed of two semi-cylindrical parts of 2.25 cm radius and 8 cm height was manufactured. This procedure is best described on the work of de Carvalho et al. [10] With this approach, it is possible to analyze the interior of the phantom by observing its inner faces (Fig. 1).

### 2.2 Heating Delivering Devices

The single element Ultrasound Therapy equipment (KLD Biosystems—AVATAR III) was previously calibrated (power and effective radiation area—ERA). The treatment parameters were adjusted to nominal intensity of  $1.0 \text{ W cm}^{-2}$  and continuous mode. The transducer was fixed in a holder and the Ultrasound Therapy equipment set to a one-minute irradiation time.

IRR Lamp equipment (Theratherm De Luxe Par 38, OSRAM, USA) has a steel bracket, with a lamp of 150 W power.

**Fig. 1** Phantom design scheme. A cylindrical PVCP phantom composed of two semi-cylindrical parts. This design was developed to allow the visualization of the internal site of the phantom immediately after heating



## 2.3 Experimental Setup

The initial temperature of the phantom (i.e. prior to heating) was set to 26 °C chosen as ambient temperature, due to the conditions of the place where the experiment was performed. Therefore, an ultrathermostat bath which consists of immersing in a reservoir that has a liquid circulation system, was used to homogeneously cool the phantom before each heating procedure.

In the Ultrasound protocol, the transducer face was placed at the top-face of the phantom and in direct contact with the gel coupling medium. Immediately after the one-minute ultrasound irradiation, the two halves of the phantom were separated to register the thermal image generated in the inner face using an Infrared Thermal Camera (IRTM) (FLIR-E63900, resolution of 0.1 °C).

In the infrared protocol, the phantom was fixed in a base positioned over the surface of the lamp distancing 30 cm from the top-face of the phantom, a recommended clinical distance. This equipment was set to irradiate for 15 min. After this time, an image of the inner faces of the phantom was immediately taken. Both the TUS and IRR positioning schemes are shown in Fig. 2.

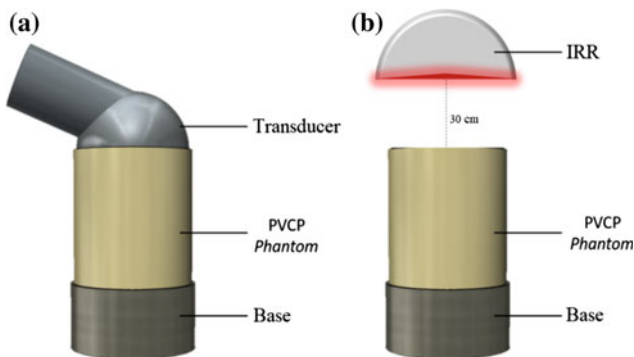


**Fig. 2** a Scheme of the 3 MHz ultrasound setup. b Scheme of the Infrared setup

The infrared camera and the holder device remained fixed in the two protocols: Ultrasound Protocol (UP) and Infrared Protocol (IP). Knowing that the lower temperature of the phantom was 26 °C and that the maximum evaluated was 50 °C, the temperature range of 20–60 °C was set at the IRTC for the experiment. To obtain the images a region with a marker was established where the phantoms were positioned.

The UP and IP protocols were performed 10 times each, totaling 20 experiments and thus 20 thermal images.

## 2.4 Image Analysis

The phantom internal faces images, Fig. 3, were obtained in grayscale by IRTC and analyzed with the aid of the MATLAB® software (MathWorks, Natick, MA, USA). First of all, a histogram of the temperature distribution on the inner faces of the phantom is obtained. Then, the most common temperature (MCT) and the maximum temperature can be observed, Fig. 4.

Only the histogram is not sufficient to extract all relevant information from the image. To understand how this temperature is distributed on the inner faces of the phantom, a 3-D graph of temperature level curves was plotted following the width and depth coordinates of the image (Fig. 5).

With this information, it is possible to study the heating patterns of the US in comparison to the IRR.

## 3 Results

The maximum temperature of each phantom was extracted from the thermal camera images by analyzing the temperature histogram distribution ( $n = 10$ ). A representative thermographic image of each protocol is shown in Fig. 6. The mean of these temperatures was calculated for UP and IP, obtaining the mean and the standard deviation of  $38.9 \pm 1.0$  and  $45.5 \pm 2.1$  respectively.

The ambient temperature assigned to the experiment was 26 °C. Therefore, it is expected that the MCT (i.e. the temperature that appears most times in the image) is close to

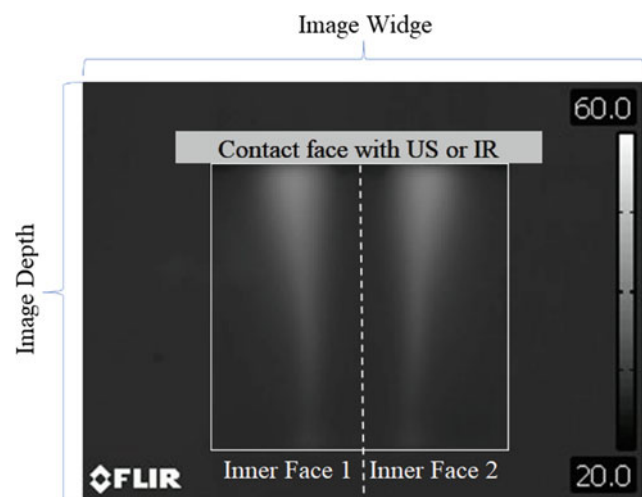


**Fig. 3** Phantom inner faces grayscale image obtained by an Infrared Thermal Camera after US radiation. The two inner faces are displayed side by side, and the upper face is the one in contact (UST) or aligned (IRR) to the thermal emitter

**Fig. 4** Histogram distribution of the temperature on the inner face of the phantom. The ambient temperature is displayed in a red line. The most common temperature (MCT), and the maximum temperature are indicated by arrows

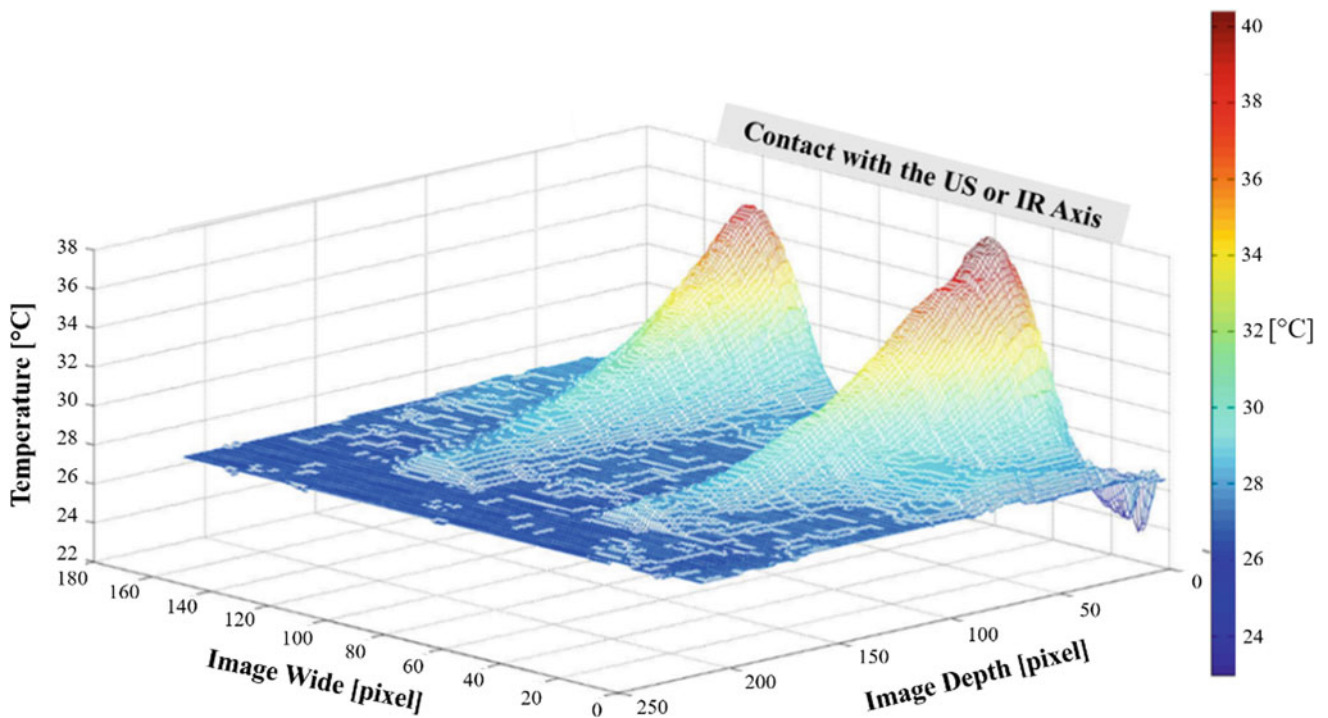
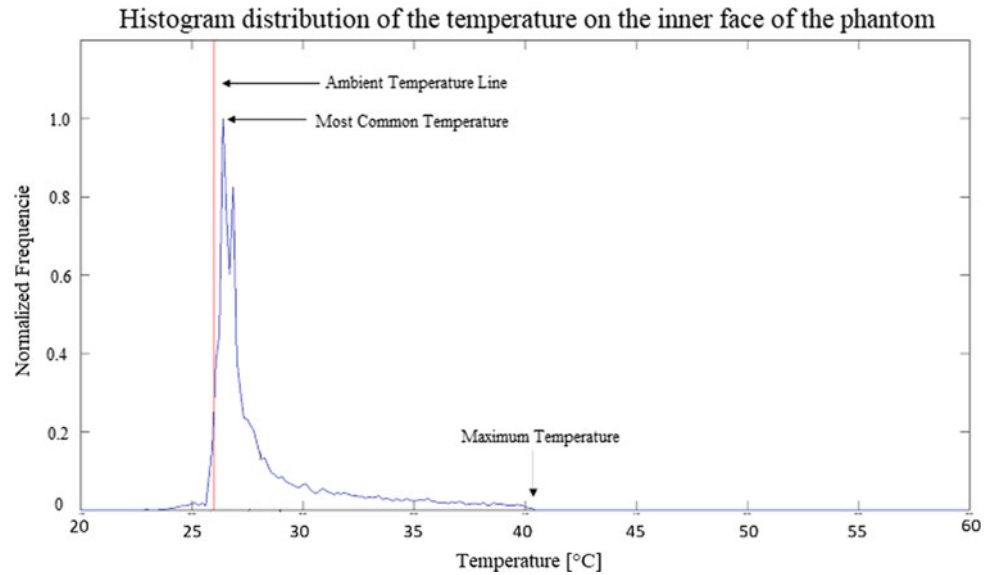


**Fig. 5** Representative temperature level curves of the two inner faces of the phantom when heated by the US

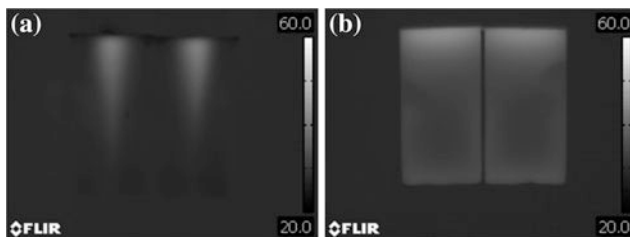
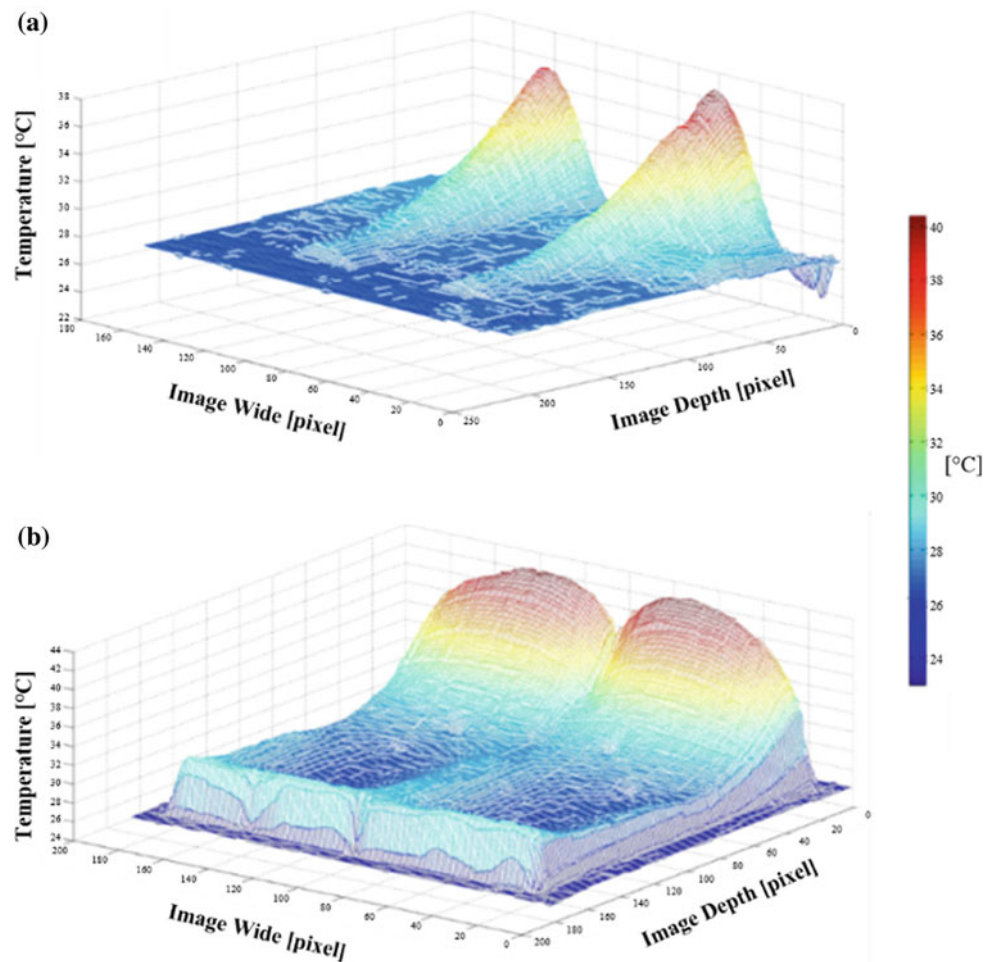


**Fig. 6** Grayscale images. **a** Internal phantom face using UP. **b** Internal phantom face using IP

this value, as US and IR radiations do not heat the whole phantom. The MCT from each heating procedure was obtained, and the mean and standard deviation of the UP phantoms,  $26.5 \pm 0.2$ , and the IP phantoms  $26.9 \pm 0.9$  was calculated for the whole inner superficies. After delimiting the analysis to heating area, were  $34.8 \pm 1.2$  and  $41.4 \pm 1.6$  for UP and IP, respectively. Those averages were obtained from the analysis of the two inner faces separately, thus being 20 images of 10 phantoms.



**Fig. 7** **a** Level curve of the UP temperature distribution. **b** Level curve of the IP temperature distribution



In the mesh analysis (Fig. 7), a graph with the temperature distribution level curve pattern at the phantom surface was generated. For the UP, it is possible to observe a more conical image, with a declining temperature curve similar to a soft exponential decay. For the IP, the temperature shows a curve also similar an exponential decay, but the area covered by IP at the surface of the phantoms is larger than for the UP.

#### 4 Discussion

After the images were acquired, a histogram of the temperature distribution was obtained from the inner faces of the phantom. The histogram displays the maximum temperature, the most common temperature (MCT), and the ambient temperature cutoff. The mean MCT was  $26.5 \pm 0.2$  for UP and  $26.9 \pm 0.9$  for IP, indicating that the phantoms were close to the ambient temperature. Although the representative image of the IP appears clearer than that of the UP, the data show that both have the MCT close to  $26.5$  °C; but the IP with a standard deviation greater than UP. Yet, when

analyzing the coefficient of variation, it is clear that the variation is low and does not exceed 3.4% for IP. When analyzing the heated area of the phantom were  $34.8 \pm 1.2$  for the UP and  $41.4 \pm 1.6$  for the IP. Those results are close to the maximum temperature, showing that the heating is well distributed into the region.

The mean maximum temperature of the phantoms was  $38.9 \pm 1.0$  °C for UP and  $45.51 \pm 2.1$  °C for IP. As can be observed, the mean was higher for infrared heating. However, we have to take some factors into account that interfere with these results. One is the time duration of application. In the UP, the time selected was 1 min (i.e., less than the time commonly used in clinical practice, 5–10 min, due to the static placement of the transducer during the whole process and thus avoiding phantom overheating [11]). The application time over IP was 15 min, this time was selected based on the clinical practices [8]. Another factor is the distance between the phantom and the infrared lamp. This distance interferes in the amount of energy received by the phantom and thus in the heating of the same. However, the recommended clinical distance of 30 cm was applied. To go

beyond the experimental setup in explaining the mean maximum temperature, the pattern of heating and deposition of energy should be studied.

To analyze the heating patterns, grayscale images were obtained from the inner faces of the phantoms. The lighter regions represent the heating area inside the phantom. It can be observed that in the UP the center of the image concentrates more heat than at the top edge, and it goes tapering along the phantom. One can observe a darker line at the top edge of the phantom (Fig. 6) that is due to the lower temperature of the ultrasonic coupling gel in contact with this region. That information is displayed by the level curve of the temperature distribution in Fig. 7. In the IP, the heating region is predominantly distributed by the surface of the phantom (i.e. at the top edge of the image, on the radiation incidence surface). However, one can note the brighter side at the edges of the phantom image, caused by the incidence of infrared in these regions that were unprotected during the heating process, since the lamp has an emission area larger than the top incident area of the phantom.

At the 3-D graphics, a temperature distribution curve can be observed on the inner surface of the phantom. In the UP, the image shows a more conical shape indicating a heating peak in the central axis of the phantom. This peak is similar on both sides, thus showing the centering of the transducer during the application. In the IP, the image shows a full-face heating caused by the radiation, as can also be seen in the grayscale image at Fig. 3. The heating is also larger at the edges and along the phantom. This heating at the edges may be due to the radiation coming from the sides of the phantom, since the lamp has an emission area larger than the top incident area of the phantom, as already mentioned.

After comparing the heating between the UP and IP protocols, one can observe that the IRR predominantly heated the top surface of the phantom directly irradiated by the lamp. The heat was probably transferred to the deeper and adjacent layers by conduction. At the TUS at 3 MHz, the heating was deeper than the IRR, and also predominantly along the propagation axis of the ultrasonic beam, (i.e. in the central region of the phantom). Therefore, during the therapeutic protocol, the choice of the equipment can be guided by the necessary heating depth of the aimed tissue. Thus, TUS for deeper tissue and IRR for superficial ones.

## 5 Conclusion

The heat generated by the TUS at the PVCP phantom was more focused and reached deeper regions, slight affecting the surface when compared to the IRR. In contrast, IRR had a

uniform concentrated heating pattern at the surface. The temperatures obtained can be adjusted by changing the protocol exposure time. However, the heating pattern contributes to understand the differences between both methods. This work proposes a new approach to superficial heating studies related to physiotherapy equipment, an area that deserves more attention of the physical principles used in the clinics, helping to clarify which method is more adequate to each clinical application.

## References

1. Florentino, D.D.M., de Sousa, F.R.A., Maiworn, A.I., de Azevedo Carvalho, A.C., Silva, K.M.: A Fisioterapia no alívio da dor: uma visão reabilitadora em cuidados paliativos. *Rev. Hosp. Univ. Pedro Ernesto*. **11** 50–57 (2012)
2. Dionísio, V.C., Volpon, J.B.: Ação do ultra-som terapêutico sobre a vascularização pós-lesão muscular experimental em coelhos. *Braz. J. Phys. Ther. Impr.* **4**, 19–25 (1999)
3. Bassoli, D.A.: Avaliação dos efeitos do ultra-som pulsado de baixa intensidade na regeneração de músculos esqueléticos com vistas à aplicabilidade em clínica fisioterapêutica, Universidade Federal do Rio de Janeiro (2001)
4. Agne, J.E.: *Eletrotermoterapia Teoria e Prática*, 1st edn. Orium (2005)
5. Mikhailenko, T.S.: A fisioterapia no tratamento de afecções articulares e tendíneas em equinos. <http://www.lume.ufrgs.br/handle/10183/119395> (2012). Accessed on 20 April 2018
6. Prentice, W.E.: *Modalidades terapêuticas para fisioterapeutas*, 4<sup>a</sup>, Mc Graw Hill, Brazil (2014)
7. Kitchen, S., Bazin, S.: *Eletroterapia prática baseada em evidências*, 11a. Manole, São Paulo (2003)
8. Lubkowska, A., Radecka, A., Bryczkowska, I., Rotter, I., Laszczyńska, M., Karakiewicz, B.: Changes in the bioelectric activity of the trapezius muscle following the thermal effect of red light and infrared radiation. *J. Back Musculoskelet. Rehabil.* (2018). <https://doi.org/10.3233/bmr-169745>
9. Omena, T.P., Costa, R.M., Maggi, L.E., Pereira, W.C.A., von Krüger, M.A.: Infrared image inside a phantom heated by ultrasound irradiation. *2011 Pan Am. Health Care Exch.* 221–221 (2011). <https://doi.org/10.1109/pahce.2011.5871887>
10. de Carvalho, I.M., Matheo, L.L.D., Júnior, J.F.S.C., de M.B.M. dos Santos, C., von Krüger, M.A., Infantosi, A.F.C., Pereira, W.C. D.A.: Polyvinyl chloride plastisol breast phantoms for ultrasound imaging. *Ultrasonics* (2016). <https://doi.org/10.1016/j.ultras.2016.04.018>
11. Omena, T.P., Costa, R.M., Pereira, W.C.D.A., von Krüger, M.A.: Calorímetro diferencial para estudo do padrão de aquecimento gerado por feixes ultrassônicos terapêuticos. *Rev. Bras. Eng. Bioméd.* **28** 355–363 (2012). <https://doi.org/10.4322/rbeb.2012.035>